Chaos, Solitons and Fractals 179 (2024) 114464

Contents lists available at ScienceDirect

Chaos, Solitons and Fractals

journal homepage: www.elsevier.com/locate/chaos

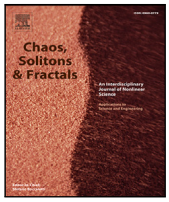

A nonlinear transient-dynamics approach to atopic dermatitis: Role of spontaneous remission

Yoseb Kang [a], Jaewoo Hwang [a], Ying-Cheng Lai [b,c], Hayoung Choi [a], Younghae Do [a,*]

[a] Department of Mathematics, Nonlinear Dynamics & Mathematical Application Center, Kyungpook National University, Daegu 41566, Republic of Korea
[b] School of Electrical, Computer and Energy Engineering, Arizona State University, Tempe, AZ 85287, USA
[c] Department of Physics, Arizona State University, Tempe, AZ 85287, USA

ARTICLE INFO

Keywords:
Atopic dermatitis
Spontaneous remission
Superpersistent scaling

ABSTRACT

Atopic dermatitis (AD) is a common skin disease that can occur in all age groups. An intriguing phenomenon associated with AD is spontaneous remission, in which the symptoms can disappear even without any treatment, especially for patients at a young age. From the point of view of dynamical evolution, spontaneous remission in AD is a transient phenomenon. A clinic implication is that, if the transient time is short, then aggressive treatment may not be necessary. A key question is thus, statistically, how long the transient time can be? Due to the lack of clinic data, mathematical modeling is a viable approach to addressing this question. Modeling AD as a nonsmooth dynamical system and regarding the disease as a transient phenomenon with spontaneous remission marking the end of the transient, we obtain a quantitative understanding of the statistical characteristics of AD. In particular, we find that, depending on the immune state, two different types of transient behaviors can arise. For type-I spontaneous remission characterized by a healthy immune level with its skin state exhibiting mild oscillations, the transient time is short, which typically occurs in patients between infancy and childhood. In contrast, type-II spontaneous remission is characterized by a low immune level and its skin state exhibits severe oscillations with a long recovering time. Quantitatively, a scaling relation exists between the average transient time (or recovery time) and some key physiological parameters, revealing that the transient is *superpersistent* in the sense that its average lifetime can diverge in a drastic way: e^{∞} as a bifurcation parameter approaches a critical value. In this case, the disease is essentially permanent, thereby requiring and justifying active treatment.

1. Introduction

Atopic dermatitis (AD) is a common, world-wide skin disease with pathogenesis originated from the complex interactions among skin barrier defects, immune response and environmental exposures including allergens and microbes. There are various phenotypes of AD that depend on sex, age and race, and this presents a significant challenge in developing effective strategies to treat the disease. Another obstacle to treatment is the lack of well-characterized animal models [1]. (For many other diseases, animal models often represent a stepping stone to clinic human treatment.) Recent years have witnessed the emergence of an interest in developing experimental approaches to pathogenesis of human AD *in vivo*, *in vitro*, and *in silico* in order to understand the underlying pathophysiological mechanisms and identify therapeutic targets and biomarkers [2,3]. Mathematical and computational models have also been developed to gain insights into the dynamical origin of AD [4–6].

A key issue in developing a human *in silico* AD model is an accurate description of the AD phenomenon. A pioneering model [5] was constructed based on the mechanisms of AD disease pathogenesis including genetic defects in the skin barrier and immune cell function on barrier dysfunction. *In silico* computational experiments for various nominal values according to human body functions related to AD [3] have led to insights into the time evolution of AD. In particular, through a dynamical analysis of AD model [5], oscillation state shown in [5] can be classified to two distinct oscillation states [6]. Finally, four stages of AD with distinct symptoms have been identified: recovery, chronic damage, mild oscillations, and severe oscillations, the combination of which has resulted in 11 AD dynamical phenotypes [6], indicating the complex nature of AD. In fact, studying AD progression in time is critical to understanding the underlying mechanisms of the disease and developing treatments. It can also help clinicians identify patients who are at risk of developing more severe forms of the disease and

* Corresponding author.
E-mail address: yhdo@knu.ac.kr (Y. Do).

https://doi.org/10.1016/j.chaos.2024.114464
Received 9 October 2023; Received in revised form 13 December 2023; Accepted 5 January 2024
Available online 13 January 2024

provide them with appropriate treatment. However, current clinical studies tend to focus on AD incidence and prevalence for different age groups [7]. For example, many studies were for infants and preschool children, because AD can disappear during infancy or childhood for a majority of these patients. Long-term follow-up studies documenting the course of AD disease and its distribution in adulthood have been rare [8]. From the real data, it is often difficult to pin down the time of recovery due to the lack of long-term tracking studies. For those reasons, *in silico* study provides an avenue to probe into the long-time behavior of AD.

A remarkable but intriguing phenomenon in the evolution of AD is that, even without any treatment, the disease can suddenly disappear, especially at a young age [8–10]. For example, patients can exhibit symptoms before the age of two but they can disappear after the age of four [11]. There are other instances in which patients suffering from AD for a long time are suddenly recovered [12,13]. This phenomenon suggests a striking feature of AD: spontaneous healing or recovery. In particular, *spontaneous remission* is referred to as an unexpected improvement or cure from a disease during its dynamical evolution. Previous works [5,6] demonstrated that, during the recovery stage with nominal skin permeability (κ_P) and certain rate of pathogen eradication by innate immune responses (α_I), spontaneous remission can always be observed [5,6]. Even for other phenotypes of AD, spontaneous remission can occur under certain initial conditions as, dynamically, AD is closely related to [6] the ubiquitous phenomenon of multistability in nonlinear dynamical systems [14–21]. While clinically, spontaneous remission is defined as the fully recovery of skin barrier integrity, different types of spontaneous remission can occur because the AD evolution depends strongly on the immune system. For example, normal skin with a strong or weak immune state can lead to relapse of AD or AD march, respectively.

What is the dynamical mechanism responsible for spontaneous remission? Answer to this question may help better understand this disease and develop more effective treatments. In this paper, we establish through mathematical modeling that AD can be understood as a dynamical transient phenomenon, with spontaneous remission marking the end of the transient. Our study reveals that, depending on the immune state, two different types of spontaneous remission can arise, as manifested by the distinct states of skin barrier, which is consistent with the findings of a previous clinical study [8]. For these two types, the patient symptoms before spontaneous remission and the recovering time are different. In particular, type-I spontaneous remission is characterized by a healthy immune level with its skin state exhibiting mild oscillations and the recovery time is relatively short. This type typically occurs in patients between infancy and childhood with early AD onset and early recovery [1,22,23]. In contrast, type-II spontaneous remission is characterized by a low immune level and its skin state exhibits severe oscillations with a long recovering time. Quantitatively, for this type, we find a scaling relation between the average transient time (or recovery time), denoted as τ_R, and a key physiological parameter – the nominal skin permeability κ_P, as

$$\tau_R \sim \exp[C(\kappa_P^* - \kappa_P)^{-n}], \tag{1}$$

where κ_P^* is a critical nominal value and $C > 0$ and $n > 0$ are constants. The most remarkable feature of this scaling relation is that, as κ_P approaches the critical value κ_P^*, the transient behavior becomes **superpersistent** [24–27] in the sense that the exponent in the exponential dependence of its lifetime diverges. This means that, for type-II spontaneous remission, there can be patients who would never recover spontaneously from AD in any practical sense – those whose skin condition is such that the permeability value is near some critical point. The implication is that, for type-II AD patients, effective treatment should be directed towards improving the skin permeability such that its nominal value is as far away from the critical value as possible.

We remark that, the phenomenon of superpersistent chaotic transients was predicted four decades ago [24] and subsequently studied in spatiotemporal physical systems [26–31]. In all the previous works, the phenomenon was studied in smooth dynamical systems. The nonlinear dynamical system underlying AD, as will be explained below, is *nonsmooth*. To our knowledge, prior to our work, superpersistent transients in nonsmooth dynamical systems had not been reported.

2. Atopic dermatitis modeled as a nonsmooth nonlinear dynamical system

Fig. 1(a) illustrates a mechanism of AD disease pathogenesis, studied by Domínguez-Hüttinger et al. [5]. External pathogens (P_{env}) enter the skin through a weak point in the skin barrier (P), but it is not a problem when the amount is small, as some pathogens die naturally. When the pathogen load exceeds P^+, physiological switches such as toll-like receptors (TLRs) and protease-activated receptor 2 (PAR2) are turned on (R_{on}). When switch R is activated, an AD flare occurs and immune substances such as antimicrobial peptides (AMP) are secreted to defend against pathogens. When an inflammatory response occurs, various signaling actions such as the secretion of cytokines induce the activation of dendritic cells (DCs), and the activated DCs migrate to the lymph nodes. In response to the switch R, kallikrein (K) becomes active, and the effect of weakening skin barrier also occurs. When the amount of P falls below P^- due to these processes, switch R is deactivated, as shown in Fig. 1(b). When switch R is activated, if the DCs of the lymph node exceed D^+, the T cells differentiate into T_H2 cells (G), and this process is irreversible, as shown in Fig. 1(c). Differentiated T_H2 cells migrate back to the epidermis and play a role in weakening the skin barrier recovery.

The mathematical model based on the dynamical interplay among skin barrier, immune regulation, and environmental stress [5] can be written as

$$\begin{aligned}
\frac{dP}{dt} &= \frac{P_{env}\cdot\kappa_p}{1+\gamma_B B(t)} - \alpha_I R(t)P(t) - \delta_p P(t),\\
\frac{dB}{dt} &= \frac{\kappa_B[1-B(t)]}{[1+\gamma_R R(t)][1+\gamma_G G(t)]} - \delta_B K(t)B(t),\\
\frac{dD}{dt} &= \kappa_D R(t) - \delta_D D(t),
\end{aligned} \tag{2}$$

where $P(t) \geq 0$, $0 \leq B(t) \leq 1$ and $D(t) \geq 0$ are the infiltrated pathogen load (in milligrams per milliliter), the strength of barrier integrity (relative to the maximum strength), and the concentration of DCs in the lymph node (cells per milliliter), respectively. Table 1 lists the relevant values of the parameters in Eq. (2) [5].

The multiscale properties of AD are captured by the switching functions describing the activation of the immune systems, as illustrated in Fig. 1, where the switches $R(t)$, $G(t)$ and $K(t)$ give the levels of the activated immune receptors, *Gata*3 transcription (relative to the maximum transcription level), and active kallikreins, respectively. These functions are [5]

$$R(t) = \begin{cases} R_{\text{off}}, \text{if } P(t) < P^- \text{or } \{P^- \leq P(t) \leq P^+,\ R(t^-) = R_{\text{off}}\}, \\ R_{\text{on}},\ \text{if } P(t) > P^+ \text{or } \{P^- \leq P(t) \leq P^+,\ R(t^-) = R_{\text{on}}\}, \end{cases} \tag{3}$$

$$K(t) = \begin{cases} K_{\text{off}}, \qquad\qquad \text{if } P(t) < P^- \text{or } \{P^- \leq P(t) \leq P^+,\ R(t^-) = R_{\text{off}}\}, \\ m_{\text{on}}P(t) - \beta, \text{if } P(t) > P^+ \text{or } \{P^- \leq P(t) \leq P^+,\ R(t^-) = R_{\text{on}}\}, \end{cases} \tag{4}$$

$$G(t) = \begin{cases} G_{\text{off}}, \text{if } D(t) < D^+ \text{ and } G(t^-) = G_{\text{off}}, \\ G_{\text{on}}, \text{if } D(t) \geq D^+ \quad \text{or } G(t^-) = G_{\text{on}}, \end{cases} \tag{5}$$

where R_{on}, R_{off}, G_{on}, G_{off} and K_{off} indicate the activating or inactivating constant level of the respective switch, but only K_{on} depends on $P(t)$: $K_{\text{on}} = m_{\text{on}}P(t) - \beta$. The two switches $R(t)$ and $K(t)$ are simultaneously activated. In particular, when $P(t)$ increases and exceeds the activation threshold value P^+, switches $R(t)$ and $K(t)$ are activated, giving rise to AD flares. However, if $P(t)$ decreases and falls below the inactivation threshold value P^-, switches $R(t)$ and $K(t)$ will be inactivated, terminating the AD flares. These behaviors indicate that

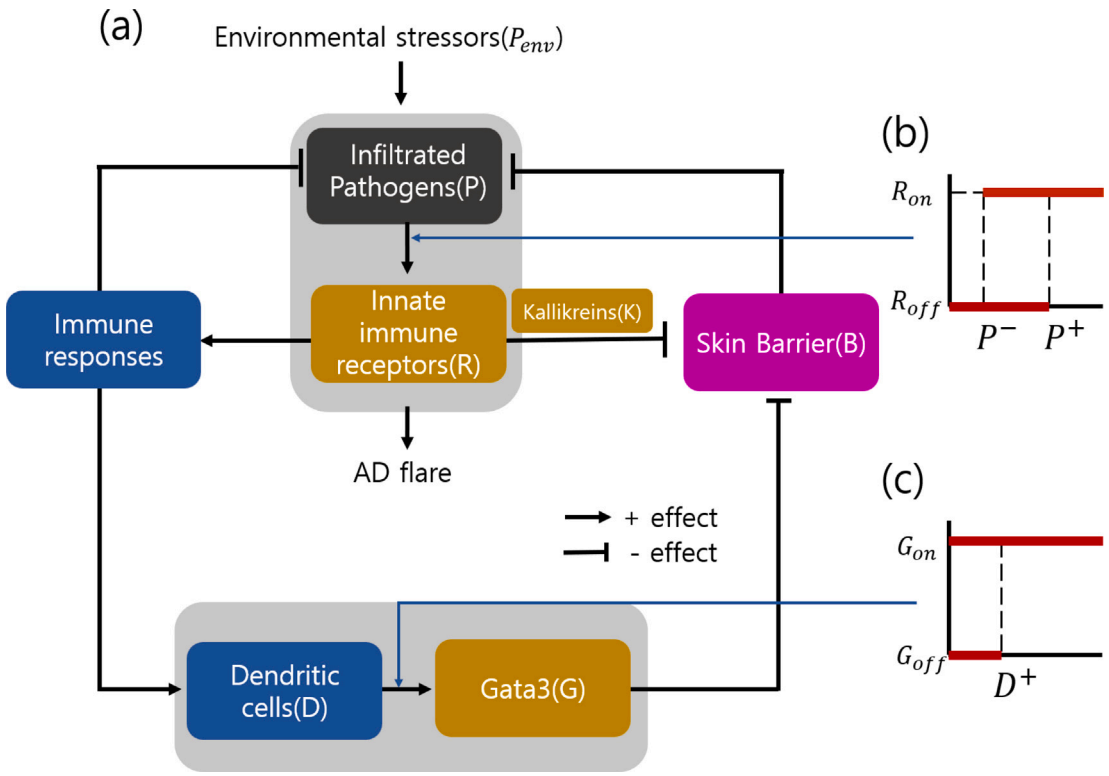

Fig. 1. Schematic illustration of atopic dermatitis process, studied by Domínguez-Hüttinger et al. [5]. (a) AD progress with switches, (b) R switch (reversible activation of innate immune receptors) and (c) G switch (irreversible *Gata*3 transcription). See text for an explanation of the role of the switches.

Table 1
Parameter values in AD system, Eq (2), are from Tab. 1 in [5].

Parameter	Description	Value
P_{env}	Environmental stress load	95 (mg/mL)
γ_B	Barrier-mediated inhibition of pathogen infiltration	1
κ_P	Nominal skin permeability	(1/day)
α_I	Rate of pathogen eradication by innate immune responses	(1/day)
δ_P	Basal pathogen death rate	1 (1/day)
κ_B	Barrier production rate	0.5 (1/day)
γ_R	Innate immunity-mediated inhibition of barrier production	10
δ_B	Rate of kallikrein-dependent barrier degradation	0.1
γ_G	Adaptive immunity-mediated inhibition of barrier production	1
κ_D	Rate of DC activation by receptors	4 cells/(mL 3 day)
δ_D	Rate of DC degradation	0.5 (1/day)
P^-	Receptor inactivation threshold	26.6 (mg/mL)
P^+	Receptor activation threshold	40 (mg/mL)
D^+	*Gata*3 activation threshold	85 (cells/mL)
R_{off}	Receptor off level	0
R_{on}	Receptor on level	16.7
G_{off}	*Gata*3 off level	0
G_{on}	*Gata*3 on level	1
K_{off}	Kallikrein off level	0
m_{on}	Slope of the linear relation between $P(t)$ and K_{on}	0.45
β_{on}	Y-intercept of the linear relation between $P(t)$ and K_{on}	6.71

$R(t)$ and $K(t)$ are *hysteretic* switches. Once $D(t)$ increases beyond the threshold value D^+ or the level of *Gata*3 activation, switch $G(t)$ is on and remains on, even when $D(t)$ decreases, so $G(t)$ is an *irreversible* switch.

So far, in *in silico* research on AD, Domínguez-Hüttinger et al. [5] had developed the mathematical model, Eq. (2), including multiscale properties of AD, which are represented by three switches. From a mathematical point of view, this AD model is nonsmooth. A nonsmooth dynamical system is a system that requires much development in theory and numerical computation. Even in study of using the same AD model, Eq. (2), with the parameter values listed in Table 1, the four clinically observed AD symptoms are identified by a classification of two distinct oscillation states: recovery (denoted as $\mathcal{R}$), mild oscillation ($\mathcal{O}_m$), severe oscillation ($\mathcal{O}_S$), and chronic damage (C) [6]. The mild and severe oscillations can be defined as the oscillation with off/on states of G-switch, respectively. Examining the onset conditions of the four AD symptoms leads to 11 AD phenotypes associated with different combinations of the symptoms [6]. In addition, the codimension-two bifurcation diagram (Fig. 2) displaying 11 AD phenotypes shown in [6] contains many different dynamical properties of AD, whose many properties are still *hidden*. That is, the codimension-two bifurcation is a hidden treasure chest in AD dynamical research. In this paper, we reinvestigate the two-dimensional parameter plane (κ_P, α_I) generating the 11 phenotypes found by Kang et al. [6] and replot it in Fig. 2. Based on Fig. 2, we will investigate spontaneous remission phenomenon of AD in Section 3.

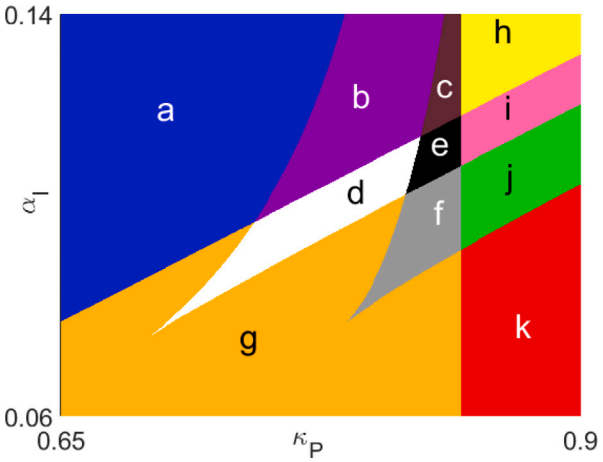

Fig. 2. Codimension-two bifurcation diagram displaying 11 AD phenotypes shown in [6]. The phenotypes are shown in alphabetic order: (a) Recovery $\mathcal{R}$, (b) ($\mathcal{R}$, $\mathcal{O}_s$), (c) ($\mathcal{R}$, $\mathcal{O}_m$, $\mathcal{O}_s$), (d) ($\mathcal{R}$, $\mathcal{O}_s$, C), (e) ($\mathcal{R}$, $\mathcal{O}_m$, $\mathcal{O}_s$, C), (f) ($\mathcal{R}$, $\mathcal{O}_m$, C), (g) ($\mathcal{R}$, C), (h) ($\mathcal{O}_m$, $\mathcal{O}_s$), (i) ($\mathcal{O}_m$, $\mathcal{O}_s$, C), (j) ($\mathcal{O}_m$, C), and (k) Chronic damage C. (For interpretation of the references to color in this figure legend, the reader is referred to the web version of this article.)

3. Results

Spontaneous remission is a phenomenon in which a patient recovers from AD without any treatment. Specifically, in the Recovery region in Fig. 2 (blue color), starting from any initial condition, the system will converge to the maximal strength of barrier integrity ($B = 1$), signifying the occurrence of spontaneous remission from AD. For other phenotypes, spontaneous remission can occur but it depends on the initial condition. To study this phenomenon in a systematic manner, we focus on the Recovery region and investigate AD-states, progress and features from the *in silico* point of view. Physiological considerations stipulate the following constraints on choosing the initial conditions [6]: $0 \le P \le 1000$, $0 \le B \le 1$ and $D = 0$.

3.1. Two types of AD spontaneous remission in the recovery region

The AD system described by Eq. (2) is a nonsmooth dynamical system constituting four subsystems, in which a healthy state is associated with unity strength of skin barrier integrity ($B = 1$). To describe spontaneous remission, we consider AD-equilibrium states (or fixed points) for $B = 1$. This can be done by calculating the fixed points in each subsystem [6]. For example, two fixed points F_1 and F_2 from two different subsystems are given by [6]:

$$F_1 \equiv (P_1, B_1, D_1) = \left(\frac{P_{env}\kappa_P}{\delta_P(1+\gamma_B)}, 1, 0\right), \tag{6}$$

$$F_2 \equiv (P_2, B_2, D_2) = \left(\frac{P_{env}\kappa_P}{\delta_P(1+\gamma_B)}, 1, 0\right). \tag{7}$$

The two fixed points are identical in their respective subsystems, but the dynamical evolution towards them in the full AD system can be different, corresponding, respectively, to the *on/off* states of the G-switch. An example of the time evolution of B is shown in Fig. 3(a) and (b) for $\kappa_P = 0.7589$ and $\alpha_I = 0.11$. It can be seen that, after some time, B approaches the same fixed point corresponding to a spontaneous remission state. Fig. 3(c–f) show that the activation processes associated with the switches for the two traces of time evolution are different, especially in terms of switch G, which is "off" for the evolution in Fig. 3(a) and "on" for that in Fig. 3(b). As G underlies the *Gata3* transcription, this switch plays an important role in AD. In particular, if it is on, serious AD may occur due to external factors such as the pathogen load in the environment exceeding a threshold. These results indicate that, even if the skin barrier integrity can be recovered to a healthy state, two distinct AD states can arise.

Table 2
Characteristics of SR-1 and SR-2 for fixed $\kappa_p = 0.745$ and $\alpha_I = 0.1$.

Property	SR-1	SR-2	$\mathcal{O}_m$	$\mathcal{O}_s$
G-switch	Off	On	Off	On
Skin barrier integrity	0.0002 ~ 0.99	0.34 ~ 0.83	0.29 ~ 0.91	0.11 ~ 0.84
Recovering time	<15	≈ 422	∞	∞

Since all switches associated with the dynamical evolution converging to F_1 are off, we have $(R, K, G) = (R_{\text{off}}, K_{\text{off}}, G_{\text{off}})$. The fixed point F_1 thus represents a *healthy state* and spontaneous remission in this case is denoted as type-I (SR-1). In contrast, the evolution converging to F_2 are associated with different switch activation: $(R, K, G) = (R_{\text{off}}, K_{\text{off}}, G_{\text{on}})$, so F_2 is potentially a *dangerous state* and spontaneous remission in this case is called type-II (SR-2). Clinically, even F_2 corresponds to the maximal skin barrier integrity, due to the memory effect of the immune system, it can lead to severe skin disease.

The two fixed points, F_1 and F_2 associated with type-I and type-II spontaneous remission, are two different attractors of the system. Clinically, how relatively common are the two types? To address this question, we examine their basins of attraction. To make visualization feasible, we focus on the two-dimensional phase space region: $0 \le P \le 1000$ and $0 \le B \le 1$, systematically vary the initial conditions in this region, and identify those that lead to attractors F_1 or F_2. A representative example is shown in Fig. 3(g), where the blue and dark-blue regions are the basins of attraction of F_1 and F_2, respectively. In the blue region, the G-switch is off while it is on in the dark-blue region. Note that the two basins of attraction have similar areas, indicating that both types of spontaneous remission can occur and be clinically observed.

3.2. Spontaneously recovering time

Fig. 3(a) and (b) indicate that, preceding spontaneous remission, oscillations in the strength B of skin barrier integrity arises after the R-switch is turned on for the first time. For convenience, we refer to the time period in which the oscillations occur as the *spontaneously recovering time* and calculate the possible B values during this time period for trajectories approaching F_1 or F_2. As shown in Fig. 3(h), for SR-1, the B value changes rapidly between 0.0002 and 0.99 with time, indicating wide variations in the skin condition. However, for SR-2, the B value changes relatively slowly between 0.34 and 0.83. The skin states associated with the two types of spontaneous remission are thus distinct.

The conditions under which the two final states, F_1 and F_2, exist are the same [6]: $P_1, P_2 < P^+$. However, their stability is different. This can be seen by calculating their eigenvalues from the Jacobian matrix. We get

$$\lambda_1^1 = -\delta_p,\ \lambda_2^1 = -\kappa_B,\ \lambda_3^1 = -\delta_D \quad \text{for } F_1, \tag{8}$$

$$\lambda_1^2 = -\delta_p,\ \lambda_2^2 = -\kappa_B/(\gamma_G + 1),\ \lambda_3^2 = -\delta_D \quad \text{for } F_2, \tag{9}$$

where δ_p, κ_B, δ_D, and γ_G are positive quantities [6]. Since the eigenvalues are negative, both F_1 and F_2 are stable. However, the difference in the magnitude of the eigenvalues stipulates different "speed" of approaching spontaneous remission from AD. In particular, we have $|\lambda_2^1| > |\lambda_2^2|$, indicating that the time for AD patients with SR-2 to be recovered can be much longer than that for patients with SR-1. Numerical results of the distributions of the spontaneously recovering time for trajectories calculated from an ensemble of initial conditions in the respective basins of attraction are shown in Fig. 3(i), where it can be seen that SR-1 and SR-2 have relatively small and large time scales, respectively. Clinically, SR-1 is related to early-onset and

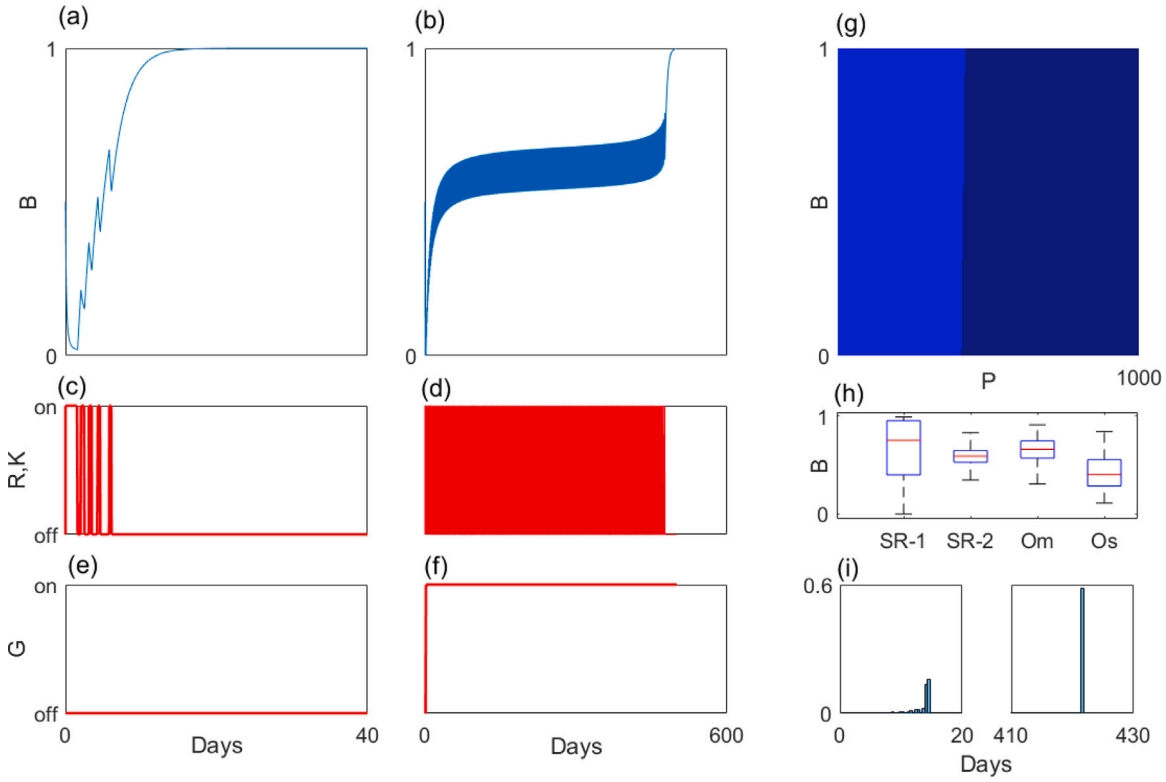

Fig. 3. Dynamical comparison of two different spontaneous remission types. For the two types, SR-1 and SR-2, (a,b) respective representative dynamical evolution, (c,d) respective activation of R- and K-switches corresponding to the time evolution in (a,b), (e,f) respective activation of G-switch. (g) Basins of attraction of the attractors associated with SR-1 and SR-2, displayed by blue and dark-blue colors, respectively. (h) Distribution of the strength of skin barrier integrity for the attractors. (i) Distribution of the recovering time for different types of spontaneous remission. Parameter values are $\kappa_P = 0.7589$ and $\alpha_I = 0.11$.

early resolving while SR-2 is associated with early-onset and late-resolving [7]. The basic characteristics of the two different spontaneous remission types are summarized in Table 2.

The two types of AD clinical symptoms [6], namely, mild oscillation $\mathcal{O}_m$ and severe oscillation $\mathcal{O}_s$, which usually require treatment, can be related to the two spontaneous-remission types, SR-1 and SR-2, respectively. There are two common features between $\mathcal{O}_m$ and SR-1: (1) their G-switch is not turned on and (2) their skin states are distributed in a similar way. In fact, the skin barrier integrity of SR-1 extends slightly beyond the range of $\mathcal{O}_m$'s skin state, indicating the protecting role played by the skin barrier of SR-1 against pathogens and in facilitating recovery. The dynamical behavior of SR-1 follows that of $\mathcal{O}_m$ for a finite time and then settles into the healthy steady state F_1 relatively abruptly. Type-I spontaneous remission can thus be regarded as a *transient behavior* from $\mathcal{O}_m$ to F_1. Likewise, the dynamical behaviors of type-II spontaneous remission and of $\mathcal{O}_s$ can be compared. As shown in Fig. 3(h) and Table 2, the distribution of skin barrier integrity for SR-2 is similar to that of $\mathcal{O}_s$ and, in both cases, the G switch is on, indicating that the skin's defense of SR-2 is weak and the recovery speed from damage is slow. Before settling into the unhealthy steady state F_2, the oscillatory behavior of SR-2 is characteristic of that of $\mathcal{O}_s$ for a finite amount of time, suggesting type-II spontaneous remission as a transient behavior from $\mathcal{O}_s$ to F_2. Taken together, the dynamics of the two spontaneous remission types SR-1 and SR-2 are both of the transient type, corresponding to mild and severe AD-clinical symptoms for a finite time, respectively, and full recovery occurs after the transient.

3.3. Scaling law for AD spontaneously recovering time

For transient dynamics, a key question concerns the average lifetime, i.e., on average, how long does it take for AD to be recovered? That is, how does the average transient lifetime τ_R depend on the bifurcation parameter? To address this question, we vary the parameter κ_P systematically and calculate the average lifetime from an ensemble of initial conditions for some typical value of α_I, e.g., $\alpha_I = 0.11$. Fig. 4(a) shows τ_R versus κ_P for the two types of spontaneous recovery, where the lifetime for SR-2 is apparently distinct from and in fact much longer than that for SR-1, $x = \kappa_P^{c1}$ and $x = \kappa_P^{c2}$ are the respective asymptotic lines for SR-1 and SR-2, respectively. The critical points $(\kappa_P, \alpha_I) = (\kappa_P^{c1}, 0.11)$ and $(\kappa_P, \alpha_I) = (\kappa_P^{c2}, 0.11)$ are located on the threshold curves of the onset conditions of mild and severe oscillation, respectively, as shown in Fig. 4(b). To assess the form of the curves in Fig. 4(a), we replot them on a logarithmic-versus-double-logarithmic scale, as shown in Fig. 4(c). The results suggest the following scaling law:

$$\tau_R \sim \exp[C(\kappa_P^{c_i} - \kappa_P)^{-n}], \tag{10}$$

where $\kappa_P^{c_i}$ is κ_P^{c1} or κ_P^{c2} for SR-1 or SR-2, respectively, and $C > 0$ and $n > 0$ are constant. The scaling law (10) is characteristic of *superpersistent* transients [24–27]. As κ_P approaches the critical value $\kappa_P^{c_i}$, the transient lifetime τ_R becomes superpersistent in the sense that the exponent in the exponential dependence diverges. The clinical implication is that it can take an extremely long time for AD patients to spontaneously recover. If the physiological conditions of the patient are such that the value of the parameter κ_P is close to the critical point $\kappa_P^{c_i}$, then the transient time can be practically infinite!

It is worth noting that the nominal value κ_P characterizes the skin permeability and is related to the skin barrier integrity. The scaling law (10) indicates that, even if the skin barrier deteriorates slightly, the spontaneously recovering time can be significantly longer. The clinical implication is that, after the onset of AD, improving the skin permeability can be effective for speeding up the recovery process.

The superpersistent scaling law (10) in fact holds for different parameter settings. Fig. 5(a) illustrates four different parameter paths.

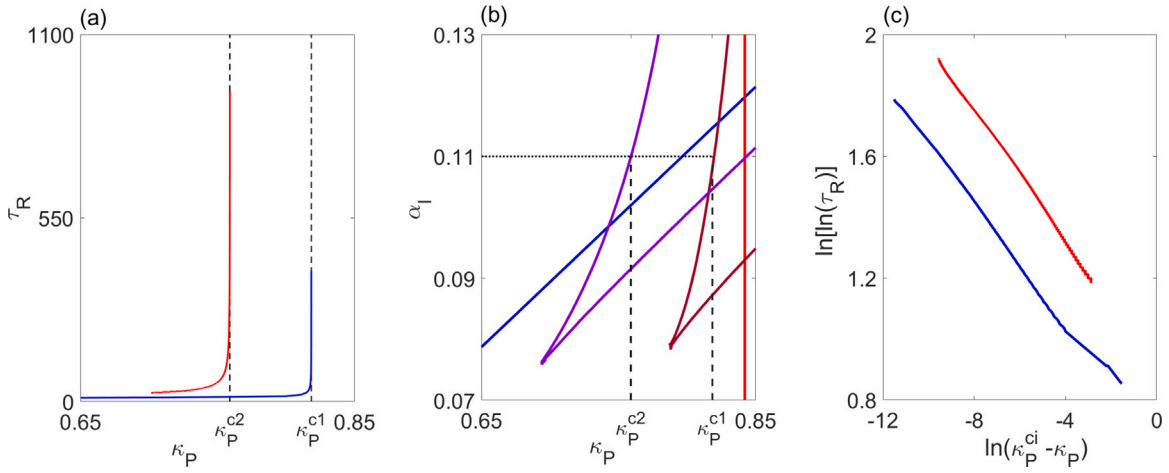

Fig. 4. Scaling law governing the spontaneously recovering time for the two types of spontaneous remission. (a) Recovering time τ_R versus κ_P for $\alpha_I = 0.11$, where the two dashed lines denote the critical points κ_P^{c1} and κ_P^{c2}, and the red and blue colors represent the recovering time for SR-2 and SR-1, respectively. (b) Threshold curves of the onset conditions of $\mathcal{R}$, $\mathcal{C}$, $\mathcal{O}_m$ and $\mathcal{O}_s$, represented by red, blue, brown and purple colors, respectively. The points $(\kappa_P, \alpha_I) = (\kappa_P^{c1}, 0.11)$ and $(\kappa_P^{c2}, 0.11)$ are marked on the threshold curves. (c) Evidence for the scaling law $\tau \sim \exp[C(\kappa_P^{ci} - \kappa_P)^{-n}]$, where $\kappa_P^{ci} = \kappa_P^{c1}$ or κ_P^{c2}.

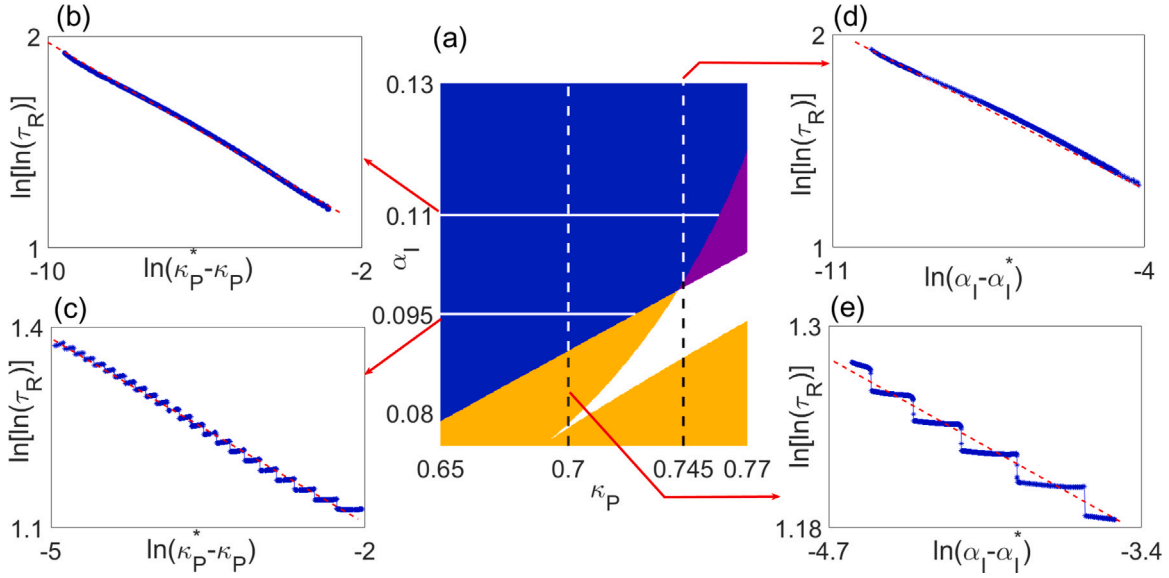

Fig. 5. Scaling law of spontaneous recovery time τ_R under different parameter settings. (a) Four different parameter paths P_i in the codimension-2 bifurcation diagram. (b–e) Scaling law governing τ_R for the four parameter paths, respectively.

For example, for $\alpha_I = 0.11$ and 0.095, which correspond to white solid lines in Fig. 5(a), the resulting scaling results of τ_R versus κ_P are shown in Fig. 5(b) and (c), respectively. Two more examples are shown in Fig. 5(d) and (e) for fixed $\kappa_P = 0.745$ and 0.7. All these results indicate the following scaling law:

$$\tau_R \sim \exp[C(\alpha_I - \alpha_I^{d_i})^{-n}], \tag{11}$$

where d_i denotes the boundary point in Fig. 5(a) where the parameter path meets.

3.4. Modulation of transient time by emollients

Emollients are substances that soften and smooth the skin through filling the gaps between the skin cells and forming a protective layer on the skin, which is often used to treat dry, itchy, or scaly skin conditions such as eczema, psoriasis, and ichthyosis. While emollients may not treat atopic dermatitis, they can effectively reduce itchiness and replenish moisture. Our question is how emollients affect spontaneous remission and the recovering time. To address this question, we consider the following mathematical model:

$$\begin{aligned}
\frac{dP}{dt} &= \frac{P_{env} \cdot \kappa_p}{1 + \gamma_B B(t)} - \alpha_I R(t) P(t) - \delta_p P(t), \\
\frac{dB}{dt} &= \frac{\kappa_B [1 - B(t)]}{[1 + \gamma_R R(t)][1 + \gamma_G G(t)]} - \delta_B K(t) B(t) + E, \\
\frac{dD}{dt} &= \kappa_D R(t) - \delta_D D(t),
\end{aligned} \tag{12}$$

where E measures the amount of emollient in conjunction with other treatments [32]. To be concrete, we fix $E = 10^{-2}$ and 10^{-3} [32], and calculate the average recovering time for the two types of spontaneous remission. The results are shown in Fig. 6(a–c). In general, applying emollient to the skin can reduce the time to spontaneous remission, as shown in Fig. 6(a). For both SR-1 and SR-2, the use of emollient can disrupt the superpersistent transient scaling law, resulting in a significant reduction in the recovery time, as can be better seen in Fig. 6(b) and (c) on a log versus double-log scale, respectively. It can be seen that application of emollient breaks the superpersistent scaling law for the spontaneous recovery time. In particular, close to the threshold

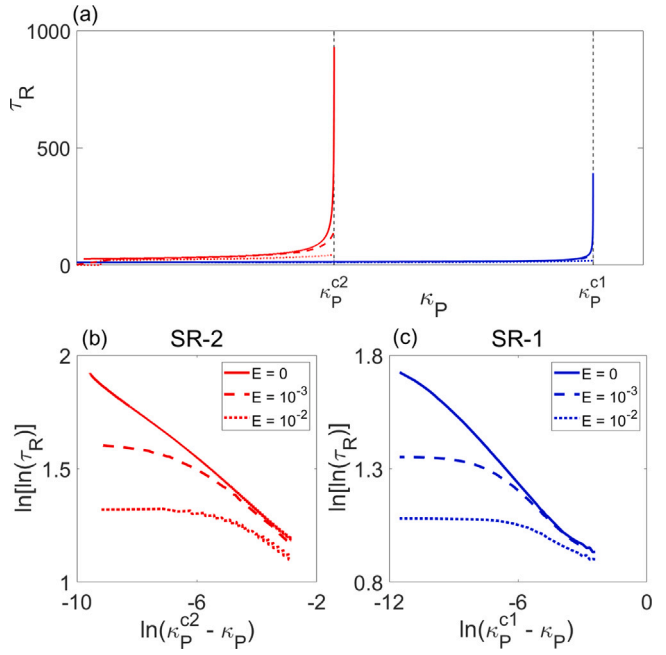

Fig. 6. Effect of emollient on the two types of spontaneous remission. (a) Recovering time τ_R versus κ_P for $E = 0$ (solid), 10^{-2} (dotted), and 10^{-3} (dashed), where the red and blue colors represent the recovering time for SR-2 and SR-1, respectively. (b,c) Scaling of the average recovering time for the two types of spontaneous remission, respectively, for different amount of emollient.

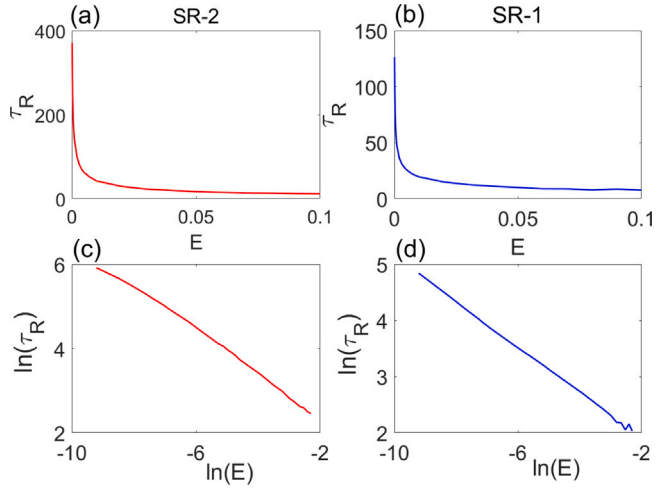

Fig. 7. Sensitivity of effect of emollient. (a,b) Recovering time τ_R versus E for $\kappa_P = 0.75898755$ (Red), 0.818440 (Blue), where the red and blue colors represent the recovering time for SR-2 and SR-1, respectively. (c,d) Scaling of the average recovering time for different amount of emollient, respectively, for the two types of spontaneous remission.

κ_P^{ci}, the recovery time τ_r is much reduced. From a clinical perspective, this result highlights the beneficial role of emollients in shortening the recovery time.

To investigate a sensitivity of emollient effect, we measure the average recovering time for different amount of emollient with fixed $\kappa_P = 0.75898755$ and 0.818440, which can be seen in Fig. 7(a) & (b), respectively. It is clear that by increasing the amount of emollient, the recovering time is significantly reduced. For a different scale, Fig. 7(a) & (b) are replotted in Fig. 7(c) & (d) on a log versus log scale, respectively, which shows that the averaging recovering time can be *exponentially* reduced by increasing the amount of emollient.

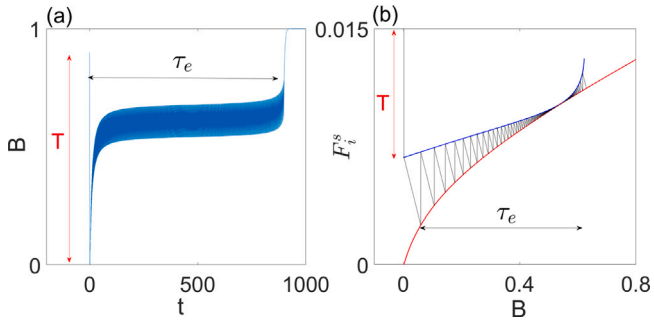

Fig. 8. AD time evolution (of B) and the corresponding slope functions. The parameter setting is $\kappa_P = 0.758978$ and $\alpha_I = 0.1100$. (a) Transient behavior and (b) the corresponding dynamical behavior of (a) transformed by the slope functions. The red and black arrows indicate the entering time T and the escape time τ_e, respectively.

3.5. Theoretical argument for AD superpersistent scaling

In smooth dynamical systems, the dynamical mechanism responsible for superpersistent chaotic transients is unstable-unstable pair bifurcation [24,25], where a pair of unstable periodic orbits coalesce with each other at the bifurcation point. The AD dynamical system described by Eqs. (2)–(5) is nonsmooth. To understand the superpersistent transient dynamics, we introduce a class of slope functions. Fig. 6(a) shows a typical time evolution of recovery, where B converges to a recovery state in a relatively abrupt manner. To understand this behavior, we consider each subsystem S_i and define a slope function F_i^s. In particular, suppose a trajectory starts from the P^- threshold line: $(P(0), B(0)) = (P^-, b)$ and $b \in (0, 1)$. There exists a time $t^* \in \mathbb{R}$ for the trajectory to reach the P^+ threshold line for the first time: $(P(t^*), B(t^*)) = (P^+, b_1)$. For each subsystem S_i, the slope F_i^s is given by the line passing through the two points (P^-, b) and (P^+, b_1):

$$F_i^s(b) = \frac{b_1 - b}{P^+ - P^-}, \text{ if the time } t^* \text{ exists.} \tag{13}$$

For instance, for the trace in Fig. 8(a), (b) shows the slope functions of S_4 (red curve) and S_2 (blue) subsystems. It can be seen that, in order for the trajectory to approach the recovery state, it must pass through the narrow tunnel formed by the two slope functions. There are two distinct time scales in this dynamical process: the time required for the trajectory to enter the tunnel (T) and the time to pass through the tunnel (τ_e), as shown in Fig. 8(a) and (b). For $\epsilon = \kappa_P^c - \kappa_P$ or $\epsilon = \alpha_I - \alpha_I^d$, the entering time follows a power law: $T \sim \epsilon^{-n}$, while the escaping time depends on the minimal distance between the two slope functions. Effectively, the minimal distance is the width of the opening of the channel, denoted as δ. Since the dynamics inside the channel are unstable, this distance increases exponentially with time. We have $\delta \sim \exp(-CT)$, where $C > 0$ is a constant. The transient time is thus given by

$$\tau \sim \frac{1}{\delta} \sim \exp[C(\kappa_P^{ci} - \kappa_P)^{-n}], \tag{14}$$

which is the scaling law characterizing superpersistent transients.

4. Discussion

A characteristic feature of AD that distinguishes it from many other diseases is that it can recover by itself – thanks to the remarkable phenomenon of spontaneous remission. From the point of view of dynamics, AD is a transient process: the system can stay in some "bad" state (AD) for a finite amount of time before approaching a "good" or healthy state. The key question is thus how long such transients can be. If the transient time is generally short on reasonable physiological time scales, then treatment may not be absolutely necessary. Clinically, short transients or speedy recovery can occur, but typically for patients

of relatively young ages. There are cases of long-lasting AD. Existing empirical data are not sufficient to give statistically reliable information about the duration of the AD, as it depends on many physiological parameters. Mathematical modeling provides a viable approach to gaining insights into AD transients and providing a quantitative characterization of their lifetime.

Due to the complexity of the dynamical system underlying AD, deriving an exact formula governing the dependence of AD transients on physiological parameters is infeasible. Nonetheless, uncovering a scaling law characterizing the leading dependence of the transient lifetime on some key parameter is possible. In this regard, it has been known that in smooth dynamical systems, a typical type of scaling of the average lifetime of chaotic transients follows an algebraic or power-law dependence on the parameter variation [33]. In this case, as the bifurcation parameter approaches the critical value, the average lifetime becomes infinite but according to some algebraic power. However, another type of transient behavior can arise: as the critical parameter value is reached, its lifetime approaches infinity in an exponential-infinite way: e^{∞} - superpersistent transient [24,25,31]. A finding of this work is that the lifetime of the AD transients follows this superpersistent scaling law. The implication is that there can be cases where the AD duration can be infinite in any realistic time scale. For those patients, treatment is necessary. We also identify a practical control/mitigation strategy to break the superpersistent scaling through, e.g., application of emollients.

In several clinical diseases, transient behavior can be observed, such as acute myeloid leukemia [34], neuroblastoma [35], metastatic melanoma [36], hepatitis [37], tuberculosis [38], and others. We hope that our research results will help understand various diseases that exhibit transient phenomena.

CRediT authorship contribution statement

Yoseb Kang: Writing – original draft, Investigation, Formal analysis. **Jaewoo Hwang:** Investigation, Formal analysis. **Ying-Cheng Lai:** Writing – review & editing, Writing – original draft, Formal analysis. **Hayoung Choi:** Investigation, Formal analysis. **Younghae Do:** Writing – review & editing, Writing – original draft, Supervision, Resources, Project administration, Investigation, Funding acquisition, Formal analysis, Conceptualization.

Declaration of competing interest

The authors declare that they have no known competing financial interests or personal relationships that could have appeared to influence the work reported in this paper.

Data availability

No data was used for the research described in the article.

Acknowledgments

This research was supported by the National Research Foundation of Korea (NRF) grant funded by the Korean government (MSIT) (No. NRF-2022R1A5A1033624 & 2022R1A2C3011711). The work at Arizona State University was supported by AFOSR under Grant No. FA9550-21-1-0438.

References

[1] Donald Y, Leung M. Atopic dermatitis: New insights and opportunities for therapeutic intervention. J Allergy Clin Immunol 2000;105:860–76.
[2] Bending D, Ono M. Interplay between the skin barrier and immune cells in patients with atopic dermatitis unraveled by means of mathematical modeling. J Allergy Clin Immunol 2017;139:1790–2.
[3] Eyerich K, Brown SJ, Perez White BE, Tanaka RJ, Bissonette R, Dhar S, Bieber T, Hijnen DJ, Guttman-Yassky E, Irvine A, Thyssen JP, Vestergaard C, Werfel T, Wollenberg A, Paller AS, Reynolds NJ. Human and computational models of atopic dermatitis: a review and perspectives by an expert panel of the international eczema council. J Allergy Clin Immunol 2019;143:36–45.
[4] Tanaka RJ, Ono M. Skin disease modeling from a mathematical perspective. J Investig Dermatol 2013;133:1472–8.
[5] Domínguez-Hüttinger E, Christodoulides P, Miyauchi K, Irvine AD, Okada-Hatakeyama M, Kubo M, Tanaka RJ. Mathematical modeling of atopic dermatitis reveals double-switch mechanisms underlying 4 common disease phenotypes. J Allergy Clin Immunol 2017;139:1861–72.e7..
[6] Kang Y, Lee EH, Kim SH, Jang B, Do Y. Complexity and multistability of a nonsmooth atopic dermatitis system. Chaos Solitons Fractals 2021;153:111575.
[7] Paternoster L, Savenije OE, Heron J, Evans DM, Vonk JM, Brunekreef B, Wijga AH, Henderson AJ, Koppelman GH, Brown SJ. Identification of atopic dermatitis subgroups in children from 2 longitudinal birth cohorts. J Allergy Clin Immunol 2018;141:964–71.
[8] Garmhausen D, Hagemann T, Bieber T, Dimitriou I, Fimmers R, Diepgen T, Novak N. Characterization of different courses of atopic dermatitis in adolescent and adult patients. Allergy 2013;68:498–506.
[9] Illi S, von Mutius E, Lau S, Nickel R, Grüber C, Niggemann B, Wahn U. The multicenter allergy study group, the natural course of atopic dermatitis from birth to age 7 years and the association with asthma. J Allergy Clin Immunol 2004;113:925–31.
[10] Bieber T, D'Erme AM, Akdis CA, Traidl-Hoffmann C, Lauener R, Schäppi G, Schmid-Grendelmeier P. Clinical phenotypes and endophenotypes of atopic dermatitis: Where are we, and where should we go? J Allergy Clin Immunol 2017;139:S58–64.
[11] Roduit C, Frei R, Depner M, Karvonen AM, Renz H, Braun-Fahrländer C, Schmausser-Hechfellner E, Pekkanen J, Riedler J, Dalphin J-C, von Mutius E, Lauener RP. The PASTURE study group, phenotypes of atopic dermatitis depending on the timing of onset and progression in childhood. JAMA Pediatr 2017;171:655–62.
[12] Rindler K, Krausgruber T, Thaler FM, Alkon N, Bangert C, Kurz H, Fortelny N, Rojahn TB, Jonak C, Griss J, Bock C, Brunner PM. Spontaneously resolved atopic dermatitis shows melanocyte and immune cell activation distinct from healthy control skin. Front Immunol 2021;12:630892.
[13] Kim YJ, Yun SJ, Lee JB, Kim SJ, Won YH, Lee SC. Four years prospective study of natural history of atopic dermatitis aged 7 8 years at an individual level: a community-based survey by dermatologists skin examination in childhood. Ann Dermatol 2016;28:684–9.
[14] Feudel U, Grebogi C, Hunt BR, Yorke JA. Map with more than 100 coexisting low-period periodic attractors. Phys Rev E 1996;54:71–81. http://dx.doi.org/10.1103/PhysRevE.54.71.
[15] Feudel U, Grebogi C. Multistability and the control of complexity. Chaos 1997;7:597–604.
[16] Feudel U, Grebogi C. Why are chaotic attractors rare in multistable systems? Phys Rev Lett 2003;91:134102. http://dx.doi.org/10.1103/PhysRevLett.91.134102.
[17] Do Y, Lai Y-C. Multistability and arithmetically period-adding bifurcations in piecewise smooth dynamical systems. Chaos 2008;18:043107.
[18] Ni X, Ying L, Lai Y-C, Do Y, Grebogi C. Complex dynamics in nanosystems. Phys Rev E 2013;87:052911. http://dx.doi.org/10.1103/PhysRevE.87.052911, URL https://link.aps.org/doi/10.1103/PhysRevE.87.052911.
[19] Patel MS, Patel U, Sen A, Sethia GC, Hens C, Dana SK, Feudel U, Showalter K, Ngonghala CN, Amritkar RE. Experimental observation of extreme multistability in an electronic system of two coupled rössler oscillators. Phys Rev E 2014;89:022918. http://dx.doi.org/10.1103/PhysRevE.89.022918.
[20] Pisarchik AN, Feudel U. Control of multistability. Phys Rep 2014;540:167–218.
[21] Lai Y-C, Grebogi C. Quasiperiodicity and suppression of multistability in nonlinear dynamical systems. Eur Phys J Special Top 2017;226:1703–19.
[22] Irvine AD, Mina-Osorio P. Disease trajectories in childhood atopic dermatitis: an update and practitioner's guide. BriT J Dermatol 2019;181:895–906.
[23] Furue M, Yamazaki S, Jimbow K, Tsuchida T, Amagai M, Tanaka T, Matsunaga K, Muto M, Morita E, Akiyama M, Soma Y, Terui T, Manabe M. Prevalence of dermatological disorders in japan: a nationwide, cross-sectional, seasonal, multicenter, hospital-based study. J Dermatol 2011;38:310–20.
[24] Grebogi C, Ott E, Yorke JA. Fractal basin boundaries, long-lived chaotic transients, and unstable-unstable pair bifurcation. Phys Rev Lett 1983;50:935–8.
[25] Lai Y-C, Grebogi C, Yorke JA, Venkataramani SC. Riddling bifurcation in chaotic dynamical systems. Phys Rev Lett 1996;77:55–8.
[26] Do Y, Lai Y-C. Superpersistent chaotic transients in physical space: Advective dynamics of inertial particles in open chaotic flows under noise. Phys Rev Lett 2003;91:224101.

[27] Do Y, Lai Y-C. Scaling laws for noise-induced superpersistent chaotic transients. Phys Rev E 2005;71:046208.
[28] Crutchfield JP, Kaneko K. Are attractors relevant to turbulence? Phys Rev Lett 1988;60:2715–8. http://dx.doi.org/10.1103/PhysRevLett.60.2715, URL https://link.aps.org/doi/10.1103/PhysRevLett.60.2715.
[29] Lai Y-C, Winslow RL. Geometric properties of the chaotic saddle responsible for supertransients in spatiotemporal chaotic systems. Phys Rev Lett 1995;74:5208–11. http://dx.doi.org/10.1103/PhysRevLett.74.5208, URL https://link.aps.org/doi/10.1103/PhysRevLett.74.5208.
[30] Tél T, Lai Y-C. Chaotic transients in spatially extended systems. Phys Rep 2008;460:245–75.
[31] Lai Y-C, Tél T. Transient chaos: complex dynamics on finite time scales. New York: Springer; 2011.
[32] Christodoulides P, Hirata Y, Domínguez-Hüttinger E, Danby SG, Cork MJ, Williams HC, Aihara K, Tanaka RJ. Computational design of treatment strategies for proactive therapy on atopic dermatitis using optimal control theory. Philos Trans R Soc A Math Phys Eng Sci 2017;375(2096):20160285.
[33] Ott E. Chaos in dynamical systems. second ed.. Cambridge UK: Cambridge University Press; 2002.
[34] Helbig D, Quesada AE, Xiao W, Roshal M, Tallman MS, Knorr DA. Spontaneous remission in a patient with acute myeloid leukemia leading to undetectable minimal residual disease. J Hematol 2020;9(1–2):18–22.
[35] Brodeur GM. Spontaneous regression of neuroblastoma. Cell Tissue Res 2018;372(2):277–86.
[36] Khosravi H, Akabane AL, Alloo A, Nazarian RM, Boland GM. Metastatic melanoma with spontaneous complete regression of a thick primary lesion. JAAD Case Rep 2016;2(6):439–41.
[37] Sato K, Kobayashi T, Yamazaki Y, Takakusagi S, Horiguchi N, Kakizaki S, Kusano M, Yamada M. Spontaneous remission of hepatitis b virus reactivation during direct-acting antiviral agent-based therapy for chronic hepatitis c. Hepatol Res 2017;47:1346–53.
[38] Lee KY, Shin C, Lee JB, Kang E-Y, Oh YW, Je BK, Choo JY, Yoon DW, Cho P-K. Spontaneously healed asymptomatic pulmonary tuberculosis: Prevalence of airflow obstruction, and correlation between high-resolution ct findings and pulmonary function tests. J Comput Assist Tomogr 2012;36(5):528–33.